1. Common Informations

DFG-Geschäftszeichen: DO 604/17-2
SCHU 729/24-2

Applicant 1:

Prof. Dr.-Ing. Michael Schütze

DECHEMA-Forschungsinstitut
Theodor-Heuss-Allee 25
D-60486 Frankfurt am Main
Germany

Tel.: +49 69 7564-337, -361
Email: schuetze@dechema.de

Applicant 2:

Prof. Dr. Reinhard Dörner

Johann Wolfgang-Goethe-Universität Frankfurt
Institut für Kernphysik
Max-von-Laue-Str. 1
60438 Frankfurt am Main
Germany

Tel.: +49 69 798 47003, -47023
Email: doerner@atom.uni-frankfurt.de

Participating individual:

Prof. Dr. Brian Martin Gleeson

University of Pittsburgh
Swanson School of Engineering
Department of Mechanical Engineering and Materials Science
648 Benedum Hall
3700 O'Hara Street
Pittsburgh, PA 15261, USA

Tel.: 001-412-648-1185
Email : bmg36@pitt.edu

Titel of the project:

Title (in German)

Aufklärung der Mechanismen der Anfangsoxidation und der Wechselwirkung mit reaktiven Elementen beim Halogeneffekt an Ni-Basislegierungen

Title (in English)

Study of the mechanisms of initial oxidation and of the interaction with reactive elements in the halogen effect for Ni-base alloys

Funding period:

1.9.2014 – 31.8.2016

List of publications:

a)

H.-E. Zschau, W. Zhao, S. Neve, B. Gleeson, M. Schütze
Promotion of the Al_2O_3-Scale Formation on Ni-Cr-Al Alloys via the Fluorine Effect
Oxidation of Metals, vol. 83 (2015), issue 3-4, 335-349.
DOI: 10.1007/s11085-014-9524-1

H.-E. Zschau, F. King, M.C. Galetz, M. Schütze
Implantation of Y- and Hf-Ions into a F-doped Ni-Base Superalloy Improving the Oxidation Resistance at High Temperatures
Nuclear Inst. and Methods in Physics Research, B 365 (2015) 202-206
DOI: 10.1016/j.nimb.2015.07.080

H.-E. Zschau, M. Schütze, M.C. Galetz, B. M. Gleeson, S. Neve, M. Lorenz, M. Grundmann
Surface Chemistry Evolution of F-doped Ni-base Superalloy upon Heat Treatment
Accepted for publication in “Materials and Corrosion”

b) no

c) no

2. Results and Discussions

The commercial Ni-base alloys with Al-contents between 3-5 wt.% are used extensively in high temperature technology. Due to the low Al content no protective alumina scale can be formed at temperatures above 900°C. Rather a fast growing complex oxide scale consisting of mixed oxides of Cr, Ni, Ti, Al and other alloying elements and spinel phases is formed [1-3]. Below this scale internal oxidation of Al leads to the formation of a non-protective inward growing alumina scale in the metal subsurface [4]. The oxide scale in fig. 1 (left image) is not able to withstand the ingress of gaseous species from the service environment. By increasing the Al content of the alloy the formation of a protective alumina scale would become possible. However a higher Al amount is detrimental for the mechanical properties. The state-of-the-art technology is covering the alloy with an Al-rich coating by e. g. CVD or PVD processes to form a protective alumina scale at high temperatures [5-8]. An alternative way is applying the halogen effect. This effect works successfully for γ-TiAl alloys. Due to the surface modification with halogens the mechanical properties of the base alloy will not be influenced.

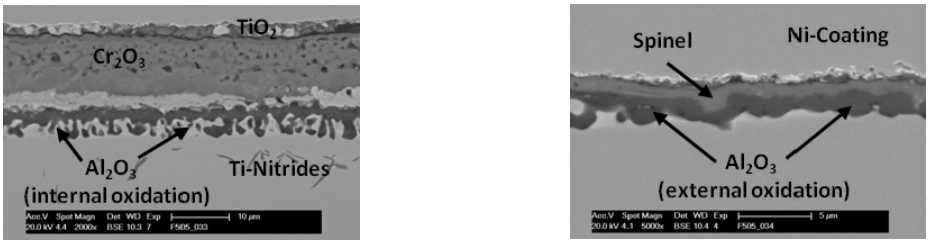

Fig 1: Left micrograph: Untreated IN738 after oxidation (24h/1050°C/air). Right micrograph: F-Implanted sample of IN738 (10^{17} F cm^{-2}/ 38 keV) after oxidation (60h/1050°C/air).

After implantation with F-ions (1 x 10^{17} F cm^{-2} / 38 keV) and isothermal oxidation (60h/1050°C/air) the oxide scale on the Ni-base superalloy IN 738 showed a change in oxidation mechanism as seen in fig. 1 (right image). An outward growing dense protective alumina scale has been formed under a spinel scale. The F-ion energy corresponds to a mean projected range of 34 nm in IN738. The optimal fluence was found to be within the values of 5 x 10^{16} and 1 x 10^{17} F cm^{-2} for an ion energy of 38 keV [9,10]. The formed protective alumina scale on IN738 remained stable and protective during isothermal oxidation (1000h/1050°C/air) [11, 12]. However, the protective alumina scale partly spalled. during cooling process, possibly due to a mismatch in CTE.

The aim of this project was to improve the adherence of the formed alumina scale by combining the halogen and the reactive element (RE) effect. It is well-known that the addition of small amounts of reactive elements (Y, Hf, Ce) leads to a good adherence of alumina (and chromia) scales [13-15]. Additionally the halogen effect should be applied to other Ni-base superalloys. Due to a long-term construction period in research lab 1 the availabilities of furnaces, of devices for metallographic and of the magnetron sputter system were limited.

We followed the recommendation of the referees to reduce the number of alloys as summarized in tab 1. The alloys PWA 1484 and Haynes 214 were delivered by lab 3.

Alloy	Ni	Co	Cr	Al	W	Mo	C	Ti	Ta	Others
PWA 1484	59,60	10,00	5,00	5,60	6,00	2,00	.	-	8,70	3 Re 0,1 Hf
IN738	61.13	9.0	16,00	3,30	1,70	2,60	0.17	3.50	1.7	0.90 Nb
RR 1000	52,4	18.5	15.00	3.00	-	5.00	0.03	3.60	2.00	0.5 Hf
Haynes 214	75.00	-	16.00	4.5	-	-	0.05	-	-	3 Fe 0.2 Si 0.5 Mn 0.1 Zr 0.01 B 0.01 Y

Table 1: Composition of the used commercial Ni-base alloys investigated (in wt.-%).

The preferred method of surface modification with F and the reactive elements Y and Hf was beam line ion implantation. This covered 2 items:

- Which **implantation sequence** (first F and second RE or vice versa) must be chosen?
- Which are the **optimal implantation parameters** (fluence, energy) and how they are connected to the concentrations of F and RE at the surface?

These investigations were carried out by using alloy IN738. The ion range of F, Y and Hf in the alloy was calculated by using SRIM [16]. The Monte Carlo-code T-DYN [17] was used for the calculation of the implantation depth profiles of F, Y and Hf in the alloy IN 738. Additionally, the depth profiles of the alloy elements Ni, Cr, Co and Al were calculated to illustrate the influence of implantation on the elemental composition near the surface.

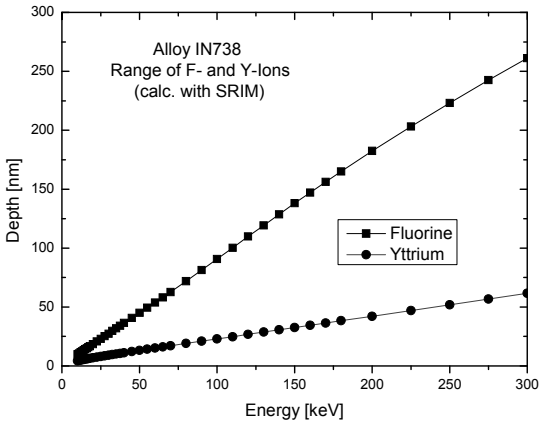

Fig 2: Range of F- and Y-ions in alloy IN 738 (calc. using SRIM [16]).

In order to meet the ion range of 34 nm for F and Y simultaneously [9-10], the corresponding ion energies were obtained from SRIM-calculations as depicted in fig. 2. In the case of the reactive element yttrium the implantations were performed with 38 keV F-ions and 110 keV Y-ions reaching a projected range of 34 nm within the alloy. For the F- and Hf-implantation F-ions of 20 keV and Hf-ions of 100 keV were used to reach a projected range of about 20 nm in IN 738.

Coupons of 10 x 10 x 1 mm^3 size were cut and polished to 4000 grit using SiC paper, followed by ultrasonically cleaning in a solution of purified water and 20% ethanol.
Implantations were carried out at the 60 kV-ion implanter of the research lab 2. For F-implantation a gas source with CF_4 was used, whereas in a sputter source Ne-gas was ionized to bombard sputter targets of pure Y and Hf. All implantations were performed on one side of the samples, whereas the other side served as a comparison. The F-profiles after the implantations were measured with non-destructive PIGE using the nuclear reaction $^{19}F(p, \alpha\gamma)^{16}O$ at a resonance energy of 484 keV. A CaF_2 – crystal served as a standard. Due to the natural line width of 0.9 keV and the proton beam energy spread, a depth resolution of about 10 nm was obtained near the surface, if an incidence angle of 60 degrees was chosen. The PIGE (Proton Induced Gamma-ray Emission) measurements were performed at the 2.5 MV Van de Graaff accelerator of the research lab 2.
Isothermal oxidation tests of the implanted specimens were carried out in lab 1 in a furnace under laboratory air using a ramp of 15 degrees per min for the heating process. When 1050°C were reached oxidation times between 72 and 144 hours were chosen. After oxidation metallographic cross-sections of all samples were prepared. Finally, all samples were analysed by metallography and SEM to study the structure and elemental composition of the oxide scale.
In [9,10] an optimum F-fluence between 5 x 10^{16} and 10^{17} F cm^{-2} was determined to form a protective alumina scale via the halogen effect for alloy IN 738. The combination of the reactive element effect and the F-effect requires a screening of the appropriate Hf-fluences to find the optimal implantation parameters for double implantation of F and Hf. In this work fluences of Hf and Y between 2 x 10^{16} and 6 x 10^{16} Hf cm^{-2} were chosen. With regard to possible losses due to ion sputtering the F-fluence of 2 x 10^{17} F cm^{-2} was also considered. Additionally, the sequence of F- and Hf-implantation must be taken into account. Prior to ion implantation Monte Carlo-calculations using the T-DYN-code allow for selection of the experimental parameters energy and fluence. After ion implantation the calculated F-depth profiles were compared with the F-depth profiles measured by PIGE, followed by metallographic cross-section preparation and analysis with SEM and ESMA.

Starting with the implantation of F (5 x 10^{16} F cm^{-2}), followed by implantation of Hf (2 x 10^{16} Hf cm^{-2}) the results of the T-DYN-simulation show that mainly the alloy elements Ni and Cr are

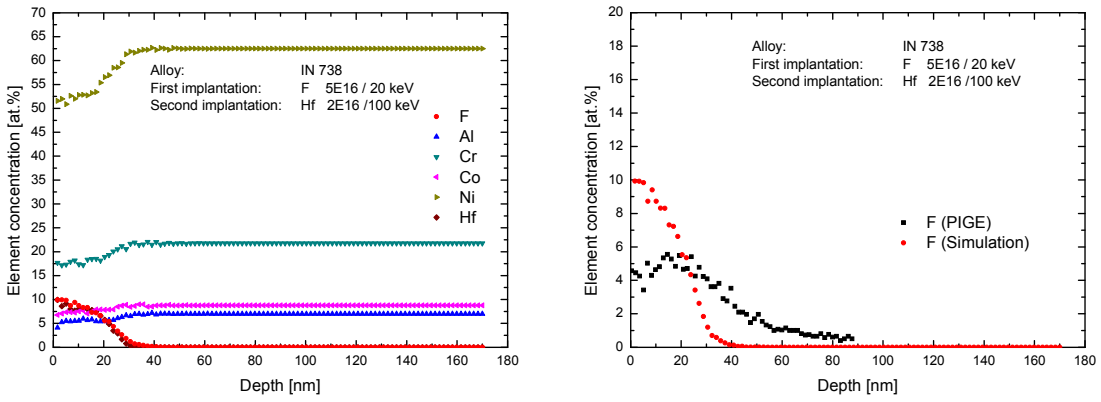

Fig 3: Left: Element profiles (T-DYN-calc.) in IN 738 after implantation of F (5 x 10^{16} F cm^{-2} / 20 keV) and of Hf (2 x 10^{16} Hf cm^{-2} /100 keV). Right: Calculated and measured F-profiles.

influenced by the implantation (figure 3). The measured F-profile reveales maximal concentrations of only 4-5 at.%. This can be explained by the sputtering of F during implantation with heavy Hf-ions. Due to the low F-amount a thin protective alumina scale of 1-2 µm was formed after oxidation only on parts of the surface as shown in the cross-section micrograph in figure 4. Mostly a non-protective oxide scale with up to 10 µm thickness (internal Al-oxidation) was formed on the surface – similar to the non-implanted side.

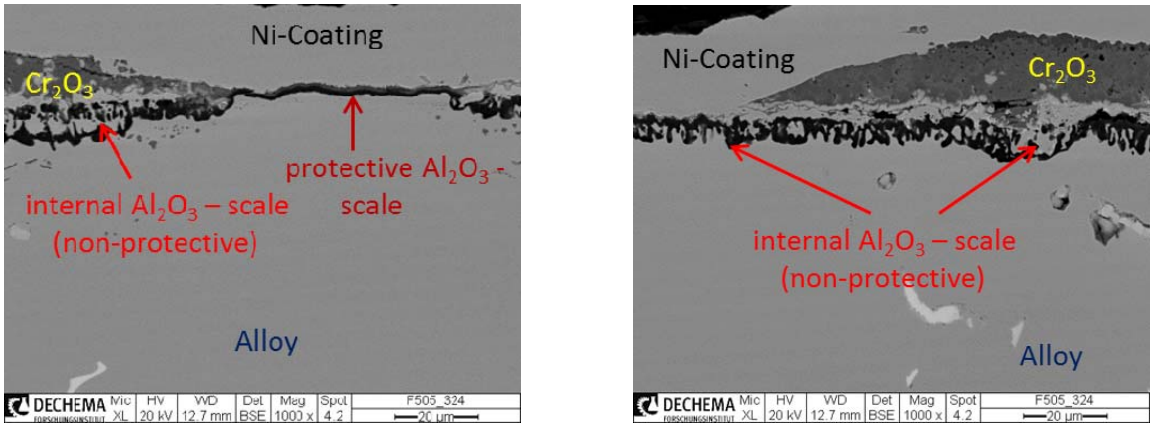

Fig 4: Cross-section of alloy IN738 from fig. 3 after oxidation (85h/1050°C/air). Left image: Implanted side. Right image: Non-implanted side.

Starting with the Hf-implantation (2 x 10^{16} Hf cm^{-2}) and followed by implantation of F (5 x 10^{16} F cm^{-2}) the maximum F-concentration reaches values of 16-18 at.% (figure 5, left image). The Hf-profile starting with 7 at.% at the surface shows a linear decrease within the range of the F-ions. Both F-profiles – calculated and measured, are in good agreement as depicted in figure 5, right image).

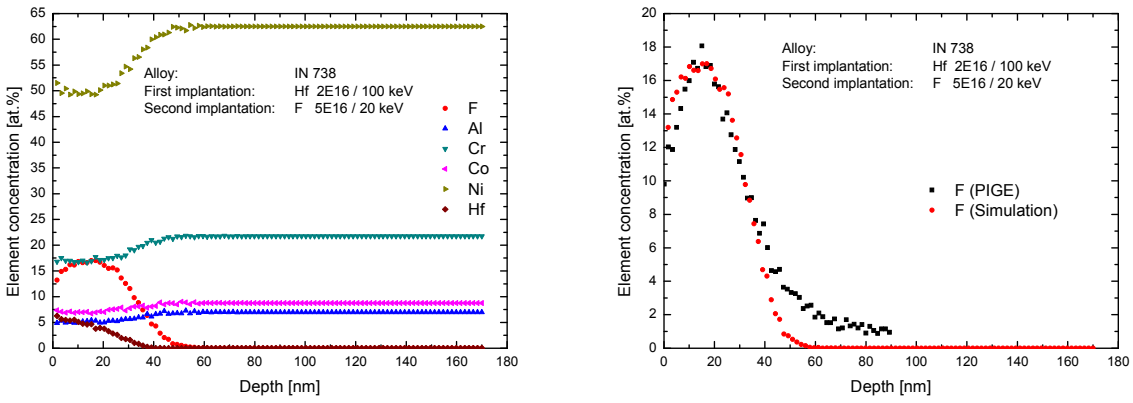

Fig 5: Left: Element profiles (T-DYN-calc.) in IN 738 after implantation of Hf (2 x 10^{16} Hf cm^{-2} / 100 keV) and of F (5 x 10^{16} Hf cm^{-2} /20 keV). Right: Calculated and measured F-profiles.

After oxidation at 1050°C the SEM micrographs reveal an adherent protective alumina scale of 1-2 µm thickness (figure 6). In contrast to this a 10 µm thick zone of internal Al-oxidation covers the surface of the untreated side. Beneath this zone a thick region of nitrides up to 20 µm has formed showing non-protective character of the internally formed alumina scale.

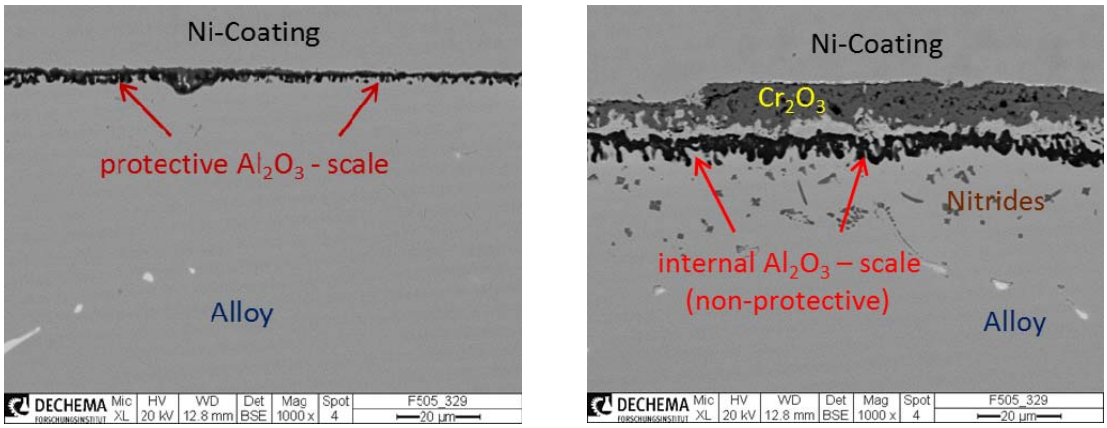

Fig 6: Cross-section of alloy IN738 from fig. 5 after oxidation (72h/1050°C/air). Left image: Implanted side. Right image: Non-implanted side.

The same implantation sequence with fluences of 4 x 10^{16} Hf cm^{-2} followed by 1 x 10^{17} F cm^{-2} leads to maximum F-amounts of 25-30 at.% (figure 7, left image) and good agreement between measured and calculated F-profiles as depicted in figure 7, right image.

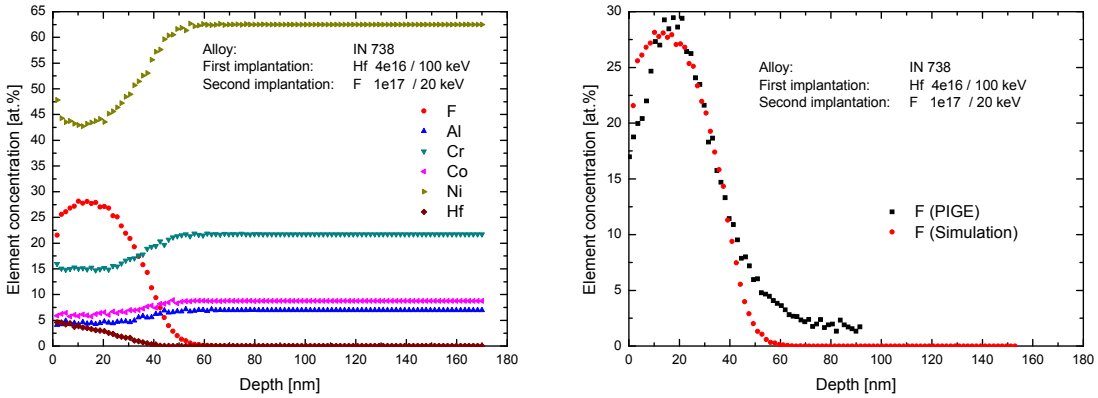

Fig 7: Left: Element profiles (T-DYN-calc.) in IN 738 after implantation of Hf (4 x 10^{16} Hf cm^{-2} / 100 keV) and of F (1 x 10^{17} F cm^{-2} /20 keV). Right: Calculated and measured F-profiles.

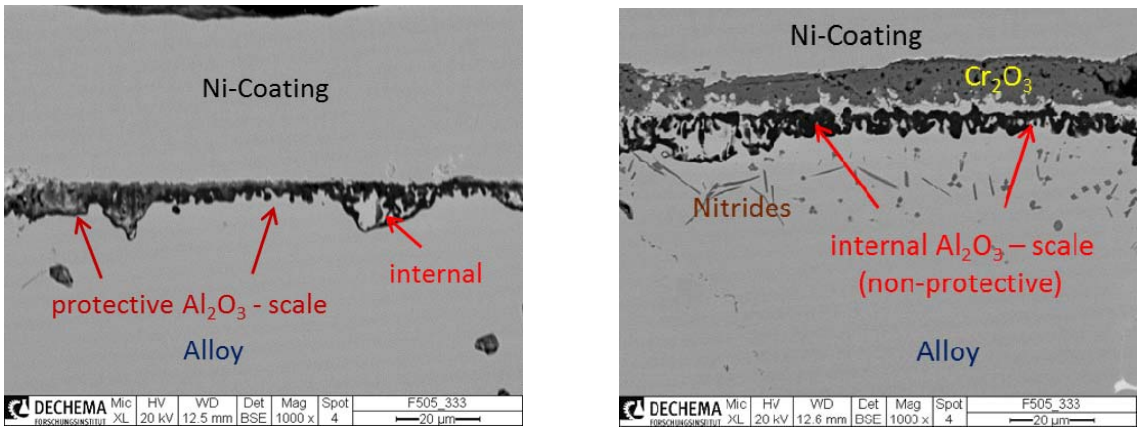

Fig 8: Cross-section of alloy IN738 from fig. 7 after oxidation (96h/1050°C/air). Left image: Implanted side. Right image: Non-implanted side.

After oxidation (96h/1050°C/air) a thin adherent alumina scale formed on the surface (figure 8). Despite a few distortions this scale also shows protective behaviour, in contrast to the non-implanted side which depicts a complex scale of chromia, internally grown alumina and nitrides.

The results obtained suggest the correct sequence of implantation: Firstly implantation of the reactive element followed by F-implantation.

By selecting the reactive element Y, a fluence of 4 x 10^{16} Y cm^{-2} and a F-fluence of 5 x 10^{16} F cm^{-2} were chosen. The calculated and measured F-profiles with maximum amounts of 12-14 at.% are in good agreement as illustrated in fig. 9. The Y-profile starting with 10 at.% at the surface can be described by a linearly decreasing function within the range of implanted fluorine.

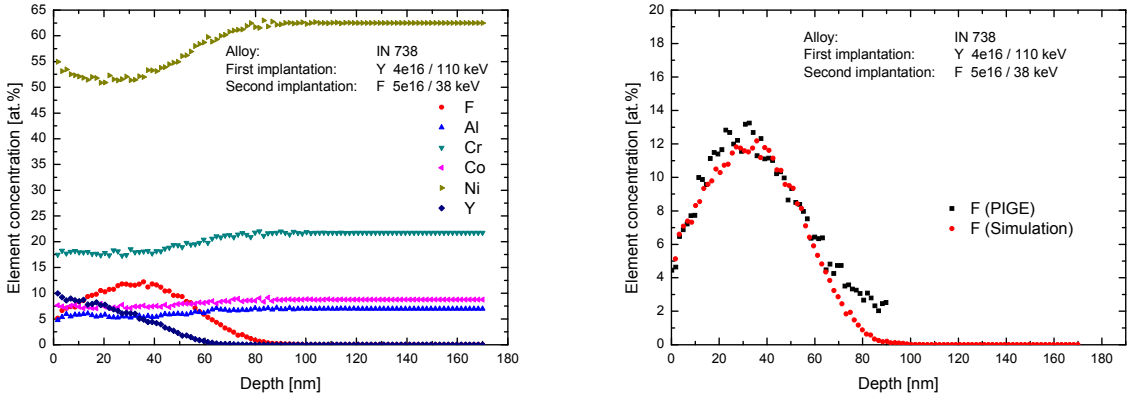

Fig 9: Left: Element profiles (T-DYN-calc.) in IN 738 after implantation of Y (4 x 10^{16} Y cm^{-2} / 110 keV) and of F (5 x 10^{16} F cm^{-2} /38 keV). Right: Calculated and measured F-profiles.

The oxide structure obtained after oxidation at 1050°C is characterised by a protective alumina scale with 1-2 µm thickness (Figure 10, left image). In contrast to this, a complex oxide scale of chromia, internally grown alumina and nitrides covers the surface of the untreated side (Figure 10, right image).

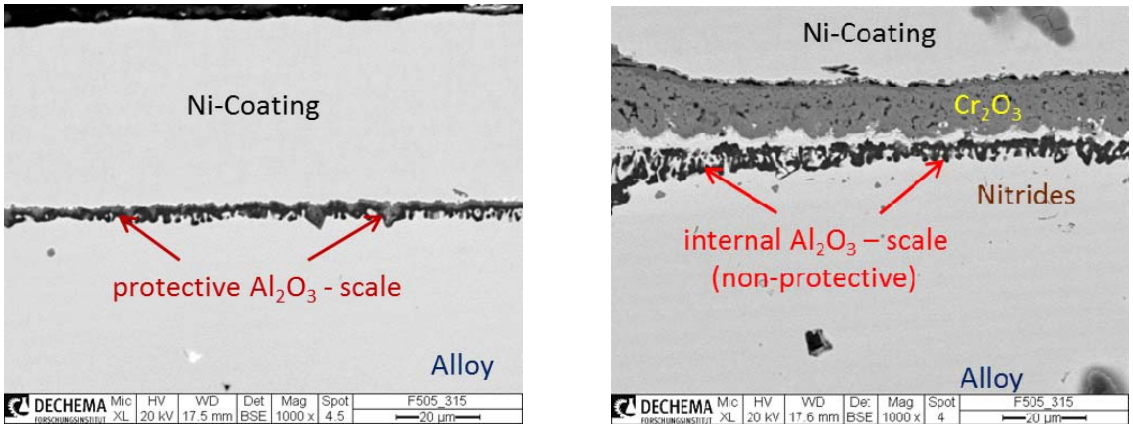

Fig 10: Cross-section of alloy IN738 from fig. 9 after oxidation (96h/1050°C/air). Left image: Implanted side. Right image: Non-implanted side.

By increasing the F-fluence to 1 x 10^{17} F cm^{-2} a maximal F-amount of about 25 at.% was obtained (fig. 11) This is a higher F-amount than predicted by the simulation leading also to a stable F-effect as has shown in [10]. In fig. 12 the elemental maps of Ni, Ti, Cr, Al, Y and

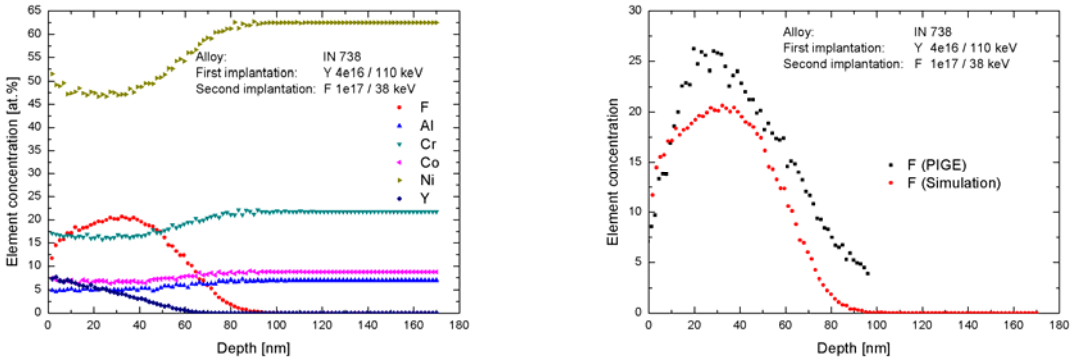

Fig 11: Left: Element profiles (T-DYN-calc.) in IN 738 after implantation of Y (4 x 10^{16} Y cm^{-2} / 110 keV) and of F (1 x 10^{17} F cm^{-2} /38 keV). Right: Calculated and measured F-profiles.

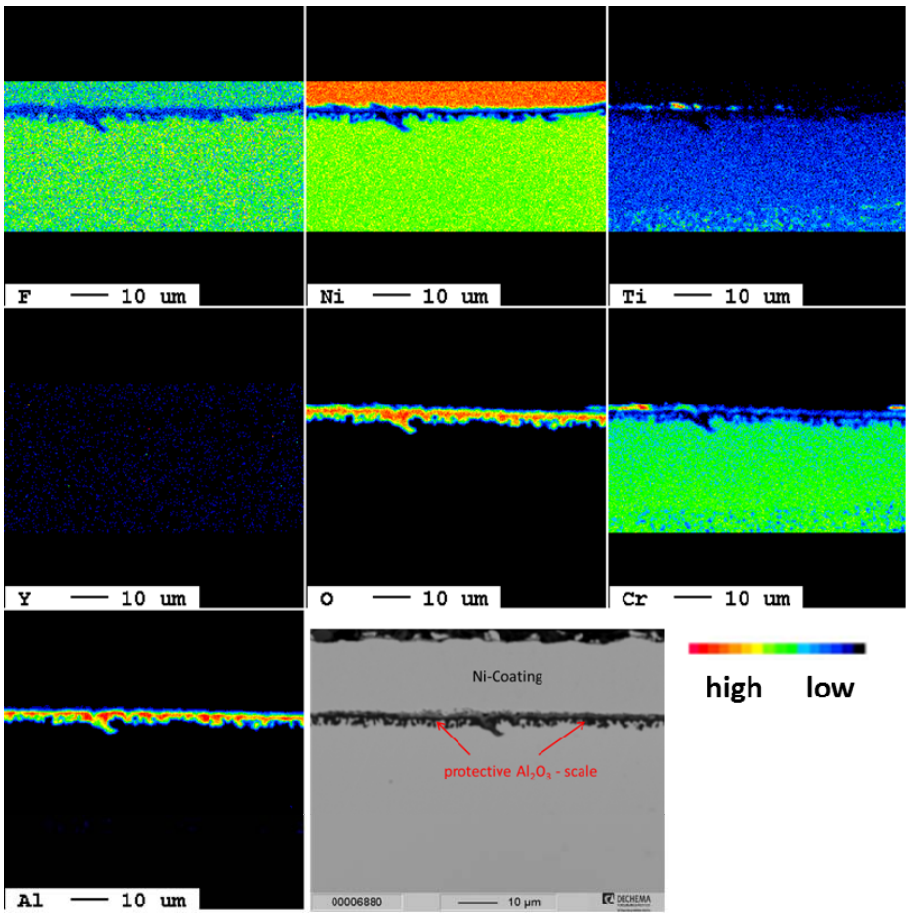

Fig 12: Elemental maps obtained with ESMA of alloy IN 738 from fig. 11 after oxidation (65h/1050°C/air).

O obtained by ESMA are displayed revealing the thin protective alumina scale formed after oxidation (65h/1050°C/air). Above this scale scales of titania and chromia are present partly. The counts of F and Y are without relevance due to a disturbance by Ni-signals.

The results suggest the correct sequence of implantation: Firstly implantation of the reactive element (heavy ion) followed by F-implantation (light ion). By doing the F-implantation firstly, the implanted F is reduced remarkably by sputtering processes during the implantation with the heavy ions Y and Hf. As optimum parameters have been found:

1. Implantation with Hf: (2 .. 4) x 10^{16} Hf cm^{-2} 2. Implantation with F: (0.5 .. 1) x 10^{17} F cm^{-2}

2. Implantation with Y: 4 x 10^{16} Y cm^{-2} 2. Implantation with F: (0.5 .. 1) x 10^{17} F cm^{-2}

These parameters were used for studying the alumina scale adherence during cyclic oxidation. For example as implantation parameters were chosen: Y (4 x 10^{16} Y cm^{-2} /110 keV) and F (5 x 10^{16} F cm^{-2} /38 keV). The oxidation started isothermally at 1050°C to establish the protective alumina scale and run under isothermal conditions. In the second

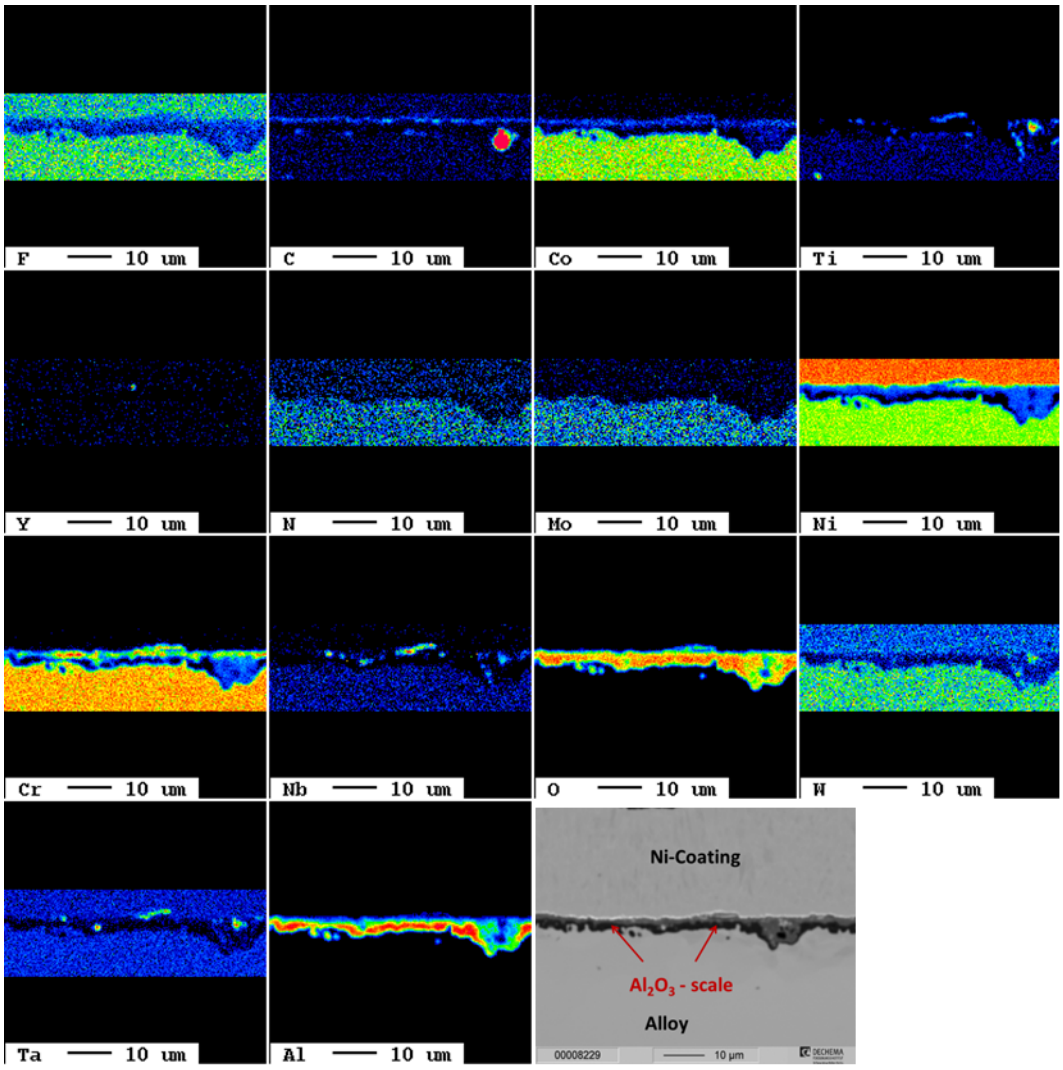

Fig 13: Elemental maps of alloy IN 738 obtained with ESMA after oxidation at 1050 °C (128.5 h isothermally and 145 h cyclically). Implantation with Y (4 x 10^{16} Y cm^{-2} / 110 keV) and F (5 x 10^{16} F cm^{-2} /38 keV). Above the protective alumina scale also titania and chromia scales are partly visible.

step the cyclic oxidation was switched on with parameters: 60 min hot dwell, 30 min cold dwell. The oxidation duration covered 128.5 h (isothermally) and 145 h (cyclically). The element maps measured with ESMA show the protective alumina scale – with some minor disturbances (fig. 13). Above the protective alumina scale of 1 µm thickness also titania and chromia scales are partly visible. These scales are brittle and often spall during cooling.

The occurrence of the halogen effect was studied also for the other commercial alloys in tab. 1. The screening was performed by implanting fluences between 10^{16} F cm^{-2} and 2 x 0^{17} F cm^{-2} at 38 keV. In the case of **RR1000** – often used as disk alloy in aero engines - no protective alumina scale was found after oxidation at 1050°C. Obviously the Al-amount in the alloy is to low.
The alloy **Haynes 214** partly forms a thin alumina scale at a temperature of 1050°C as seen in fig. 14, right image. However the 1 µm thick alumina scale at the implanted side covers the

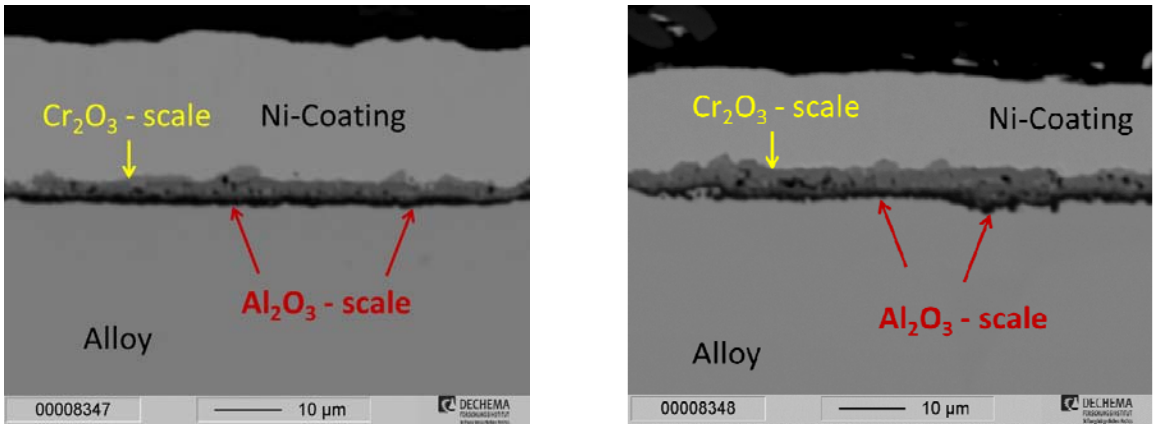

Fig 14: Cross-section of alloy Haynes 214 from fig. 9 after oxidation (73h/1050°C/air). Left image: Implanted side (5 x 10^{16} F cm^{-2} /38 keV). Right image: Non-implanted side.

whole surface. The implanted side (left image) reveals a more continuous alumina scale without inclusions of chromia than at the non-implanted side. A 2-5 µm thick chromia scale is located above the alumina scale. The good adherence of the alumina scale may be due to the presence of the minor alloying reactive element Y (see tab. 1).

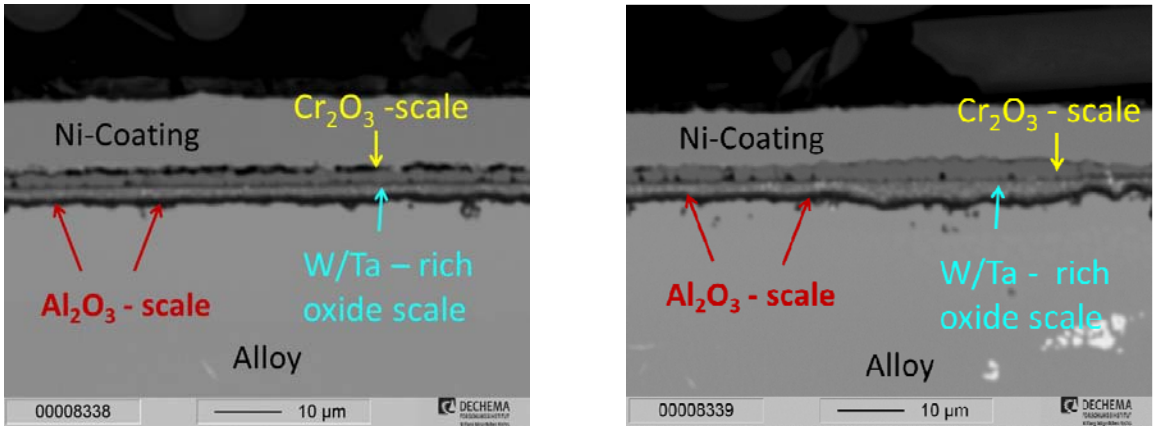

Fig 15: Cross-section of alloy PWA 1484 from fig. 9 after oxidation (72h/1050°C/air). Left image: Implanted side (1 x 10^{16} F cm^{-2} /38 keV) Right image: Non-implanted side.

No significant difference due to the F-implantation was found for the alloy PWA 1484. This alloy forms a thin adherent alumina scale covered by two scales. The inner scale contains oxides rich in W and Ta, whereas the outer scale consists. of chromia. The minor alloying reactive element Hf increases the adherence of the alumina scale

Bibliography

[1] Singheiser, L.; Steinbrech, R.; Quadakkers, W. J.; Clemens, D.; Siebert, B.; *Thermal Barrier Coatings for Gas Turbine Applications- Failure Mechanisms and Life Prediction,* 6th Liege Conference on Mat. For Adv. Power Engineering, 5-7 Oct. 1998, Liege, B, Proc. Europ. Comm., Eds. J. Lecomte-Beckers, F. Schubert, P.J. Ennis, vol. II, 977 – 996.

[2] Munoz-Arroyo, R.; Clemens, D.; Tietz, F.; Anton, R.; Quadakkers, W. J.; Singheiser, L.; *Influence of Composition and Phase Distribution on the Oxidation Behaviour of NiCoCrAlY Alloys.High Temperature Corrosion and Protection of Materials*, 22 -26 May 2000, Les Embiez, F, Materials Science Forum, Vols. 369-372, 2001, 165 – 172

[3] Li, H.; Son, X. F.; La, J. G.; Zhang, Z. Y.; Jim, T.; Guan, H. R.; Hu, Z. Q. *Oxidation Behavior of a Single-Crystal Ni-Base Superalloy in Air. I: At 800 and 900°C,* Oxidation of Metals 59, 2003, no. 5/6, 591-605

[4] Litz, J.; Rahmel, A.; Schorr, M.; Weiss, J.; *Scale Formation on the Ni-Base Superalloys IN 939 and IN 738 LC,* Oxidation of Metals, 32, 1989, 167- 184

[5] Beele, W.; Czech, N.; Quadakkers, W. J.; Stamm, W.; *Long term oxidation tests on a Re-containing MCrAlY- coating.* Abstract, International conference on Metallurgical coatings and thin films. ICMCTF 97, San Diego, 21-25 April 1997, Proceedings in Surface and Coatings Technology 94/95, 1997, 41-45

[6] Quadakkers, W. J.; Shemet, V.; Sebold D.; Anton R.; Wessel E.; Singheiser L.; *Oxidation Characteristics of a Platinized MCrAlY Bond Coat for TBC Systems during Cyclic Oxidation at 1000°C.* Surface & Coatings Technology 1, 2005, 77-82

[7] Strauss, D.; Müller, G.; Schumacher, G.; Engelko, V.; Stamm, W.; Clemens, D.; Quadakkers, W.J.; *Oxide Scale Growth on MCrAlY bond Coatings after Pulsed Electron Beam Treatment and Deposition of EBPVD-TBC.* Surface and Coatings Technology, 135, 2001, 196 – 201

[8] Toscano, J.; Vaßen, R.; Gil, A.; Subanovic, M.; Naumenko, D.; Singheiser, L.; Quadakkers, W.J.; *Parameters Affecting TGO Growth and Adherence on MCrAlY-Bond Coats for TBC's. ICMCTF-2006,* Presentation No. A1-1-4, Paper No. 785, Surface and Coatings Technology

[9] Zschau, H.-E.; Renusch, D.; Masset, P.; Schütze, M.; *A new concept of oxidation protection of Ni-base alloys by using the halogen effect*, Materials at High Temperatures 26, No. 1, 2009, 85-89

[10] Zschau, H.-E.; Renusch, D.; Masset, P.; Schütze, M.; *The halogen effect for Ni-base alloys – a new method for increasing the oxidation protection at high temperatures*, Nucl. Instr. & Meth. in Phys. Res., B 267, Issue 8-9, 2009, 1662-1665

[11] Zschau, H.-E; Renusch, D.; Masset, P. J.; Schütze, M.; *Formation of a protective alumina scale on Ni-base superalloys by using the halogen effect*, Advanced Materials Research, Vol. 278, 2011, 485-490

[12] Zschau, H.-E.; Masset, P. J.; Schütze, M.; *Oxidation protection of Ni-base superalloys by halogen treatment,* Materials and Corrosion, Vol. 62, 2011, Issue 7, 687–694

[13] Smialek, J. L.; Pint, B. A. ; *Optimizing Scale Adhesion on Single Crystal Superalloys*, Mater. Sci. Forum, 369-372, 2001, 459-466

[14] Christensen, R. J.; Tolpygo, V. K.; Clarke; D. R.; *The Influence of the Reactive Element Yttrium on the Stress in Alumina Scales forms by Oxidation*, Acta mater. Vol. 45, no. 4, 1997, 1761-1766

[15] Hou, P. Y.; *The Reactive Element Effect – Past, Present and Future,* Materials Science Forum, Vol. 696, 2011, 39-44

[16] Ziegler, J.; Biersack, J.; Littmark, U.; *The stopping and range of ions in solids, Version 95*, Pergamon Press, New York. 1995

[17] Biersack, J.; *TRIM-DYNAMIC applied to marker broadening and SIMS depth profiling,* Nucl. Instr.& Meth. in Phys. Res., B 153, 1999, 398-409

3. Summary

Ni-based superalloys with relatively low Al-contents between 3-5 at.% are often used in high temperature technology. Due to their low amount of Al these alloys are unable to form a protective alumina scale. The halogen effect – working successfully for Gamma-TiAl-alloys - offers a new way to form a protective alumina scale also for these Ni-base alloys. For the surface modification F-ion implantation was applied performing a screening to find the suitable "window" for the halogen (fluorine) effect. For alloy IN 738 a change of oxidation mechanism was achieved to form an outward growing dense protective alumina scale during oxidation at 1050°C. Also for alloy Haynes 214 the tendency to form a protective alumina scale can be supported by surface modification via fluorine ion implantation. The formed alumina scale shows a more protective structure due to a lack of inclusions like chromia. In case of alloy PWA 1484 no significant influence on scale formation was found. This alloy already forms a thin alumina scale at the metal/oxide-interface. Due to the low Al content in alloy RR1000 no protective alumina scale was found. A successful application of the halogen effect would become possible, if the surface region will be enriched with Al by e. g .CVD processes before doping the surface with fluorine.

The halogen effect was combined with the reactive element (RE) effect to improve the adherence of the thin protective alumina scale. The subsequent ion implantation with F and the RE Y and Hf showed how important the implantation sequence is. At first the RE must be implanted, followed by fluorine. As optimal implantation parameters were determined:

1. Implantation with Hf: (2 .. 4) x 10^{16} Hf cm^{-2} 2. Implantation with F: (0.5 .. 1) x 10^{17} F cm^{-2}

2. Implantation with Y: 4 x 10^{16} Y cm^{-2} 2. Implantation with F: (0.5 .. 1) x 10^{17} F cm^{-2}

Those alloys containing small amounts of reactive elements (Haynes 214, PWA 1484) reveal a suitable adherece of the alumina scale. No surface modification with RE is needed.